

# Thermal stability and oxidation resistance of novel carbon-silicon alloy fibres

S. LU, B. RAND\*

*Leeds University Carbon Centre, Department of Materials, University of Leeds,  
Leeds LS2 9JT, U.K.*

K. D. BARTLE

*Leeds University Carbon Centre, School of Chemistry, University of Leeds,  
Leeds LS2 9JT, U.K.*

The effect of thermal treatment on the properties and structure of carbon-silicon alloy fibres produced from a novel silicon-containing carbon precursor is reported. The precursor, containing about 22 wt % Si, was melt spun into fibres and then oxidatively stabilized under different conditions to render the fibres infusible. The fibres were pyrolysed and heat treated to 1600 °C in inert atmosphere. The extent of stabilization was found to be critical to the development of mechanical strength of the fibres which varied with heat treatment temperature, showing a maximum at 1200 °C when the strength was 1.2–1.4 GPa. Moduli were low because of the lack of orientation of the carbon layer planes along the fibre axis. The maximum strength and the thermal stability at high temperatures is considerably reduced if the fibres are excessively oxidized at the stabilization stage. Optimally stabilized fibres show a drop in strength at 1300 °C but this stabilizes at about 600 MPa over the range 1300–1600 °C. These strengths are remarkably good considering the low modulus which is due to the quite high failure strains. The fibres can show excellent resistance to oxidation if given an initial short exposure to oxygen at high temperature. This is considered to be due to an imperceptible layer of silica. © 1999 Kluwer Academic Publishers

## 1. Introduction

The high temperature application of carbon fibres is restricted because they are prone to oxidation at temperatures above 450 °C. There have been many attempts to protect carbon products by coatings that form oxidation barriers [1–3]. However, these coatings often crack in use, exposing the underlying carbon to the oxidizing gas [4]. High performance SiC fibres are produced from polycarbosilane precursors [5], which are very oxidation resistant and possess high mechanical properties, but their tensile strength decreases rapidly at temperatures above 1200 °C due to  $\beta$ -SiC crystallization and internal chemical reactions. A fibre system with characteristics of both carbon fibres and SiC fibres should attract new or expanded applications. It has recently been shown that polycarbosilanes can be incorporated into pitch to produce isotropic C/Si alloy fibres with useful mechanical properties [6]. Precise control of the fibre stabilization process is essential to optimize the mechanical properties of both the stabilized and pyrolysed fibres as is the case with the carbon fibres [7]. This paper reports the improved mechanical properties of the CSA fibres obtained by this process, with the emphasis on the pyrolysis and controlled oxidation processes, and shows how these novel carbon fibres, alloyed with

silicon, have in-situ oxidation resistance enabling them to generate and regenerate protective outer layers.

It has been established that novel oxidation-resistant carbon-silicon alloy (CSA) fibres could be produced by reacting polysilane species with pitch molecules, melt-spinning the resultant precursor into fibres which were then subjected to oxidative stabilization, pyrolysis and controlled oxidation. The fibres were structurally isotropic and their mechanical properties were similar to those of general purpose isotropic pitch-based carbon fibres (strength: 400–600 MPa, modulus: 30–40 GPa) [6]. These properties can be more than doubled by controlling the extent of stabilization so that it is sufficiently high to provide infusibility during the ensuing pyrolysis to the CSA fibres, but under conditions that avoid excessive oxidation to gaseous products, enabling the mechanical properties for both stabilized fibres and pyrolysed fibres to be optimized [7].

## 2. Experimental

The silicon-containing precursor was prepared by extracting a petroleum pitch Ashland A240 with toluene and reacting the soluble fraction with polydimethylsilane (weight ratio = 1 : 1) in a synthesis reaction

\* Corresponding author. Fax: 0113 242 2531; e-mail b.rand@sun.leeds.ac.uk.

system [6]. The reactor was constructed to promote reactions both in the liquid phase (440 °C) and in the gaseous phase (650 °C) involving recycling conditions at atmospheric nitrogen pressure. The reaction product was distilled under vacuum to remove the low boiling point light fraction. The vacuum distilled product was used as the spinning precursor in the production of fibres. The spinning precursor has a silicon content of 22.1 wt% and a softening point of 290 °C (estimated by hot-stage microscopy). As a fibre spinning precursor, a high carbon-ceramic yield is required, combined with good fluidity below the decomposition temperature ( $T_{0.5}$ ).  $T_{0.5}$  is defined here as the temperature at which the spinning precursor loses 0.5% in weight.  $T_{0.5}$  sets the upper limit for the spinning temperature in order to prevent significant chemical change during this thermoforming process.

The spinning precursor was formed into fibre by melt-spinning at 340 °C. The precursor melt, with appropriate rheological characteristics at the spinning temperature, was extruded through a single hole spinneret ( $D = 0.25$  mm,  $L/D = 2$ ). With proper drawdown of the viscous precursor melt during extrusion from the spinneret, fibres with diameter of 10–15  $\mu\text{m}$  were produced. A drum on a variable speed motor was used for fibre take-up.

The fibres were oxidatively stabilized by heating in air or oxygen to the weight gains of 4.5 wt% and 10 wt% respectively, to investigate the influence of the extent of oxidation on the mechanical properties of the fibres. The stabilized fibres were pyrolysed at a heating rate of 100 °C/hr to various temperatures (up to 1600 °C) under an argon atmosphere, which was maintained for 2 hours.

The tensile properties of pyrolysed fibres were measured using a universal testing machine, Instron 1185. Measurements were made with gauge length of 20 mm, using a crosshead speed of 0.2 mm/min. About 30 fibres of each type were tested. The broken fibre ends were numbered and saved for diameter measurements using a CAMSCAN Series 3 SEM. The diameters of both fibre ends were measured and the average of the two was taken as the fibre diameter (It should be noted that in many cases, especially for more brittle fibres, the fibre ends examined may not have been the actual primary fracture surfaces, due to secondary or tertiary fractures). Using the diameter measured by SEM, the individual fibre tensile strength, Young's modulus and elongation were calculated from the load-displacement curves. The average values were taken as the tensile properties of the fibres.

Carbon, hydrogen, nitrogen and sulphur contents were determined by ultimate analysis. Silicon was analysed by atomic absorption spectrophotometry. The oxygen content was obtained by difference.

Infrared spectra were recorded on a Perkin Elmer FTIR Spectrometer 1725X, using KBr pellets containing about 1 wt% of powdered samples.

$^{13}\text{C}$  and  $^{29}\text{Si}$  NMR spectra were recorded on a solid state NMR system consisting of a Varian Unity plus spectrometer (300 MHz for protons) and Doty Scientific probe with cross-polarization (CP) and magic-angle sample spinning (MAS). The powdered sample

was packed into a ceramic capsule, which was spun and examined at 75.4 MHz for carbon and 59.6 MHz for silicon.

X-ray diffraction measurements were performed by a Philips APD 1700 diffractometer using nickel filtered copper  $K\alpha$  X-rays which have a wavelength of 0.1541 nm. The powder samples were prepared by crushing fibres with an agate mortar and pestle. The powders were then mounted on a flat glass holder, which has a round opening of diameter  $\sim 10$  mm. The specimens were scanned over the  $2\theta$  range from 5° to 90°. The (111) peak corresponding to  $\beta$ -silicon carbide was used for estimating the crystallite size of this phase. A scan size of 0.01° and a scan rate of 0.01°  $\text{s}^{-1}$  were used.

The electrical resistance of fibres was measured by a multimeter (8050A). Six fibres were measured and the average value was used to calculate the resistivity.

The oxidation resistance was assessed in air in a Stanton R-01 thermobalance. In each measurement, 50–90 mg (depending on the overall weight loss) of sample was used. It was heated from ambient to 1000 °C at a heating rate of 5 °C/min.

### 3. Results and discussion

#### 3.1. Structural changes during the pyrolysis of fibres with different extent of stabilization

It has been shown that the early stage of the pyrolysis process (400 °C–800 °C) involves the elimination of alkyl groups, carboxyl, carbonyl and Si-O bridging structures, converting the organopolymeric precursor into an amorphous brittle inorganic carbon-silicon alloy [6]. However, it is very difficult to investigate the Si-O structures by FTIR since the bands located in the region of 800–1100  $\text{cm}^{-1}$  overlap with those for Si-CH<sub>3</sub> stretching modes and aromatic out-of-plane C-H bending modes. The solid state NMR technique provides an alternative.

Fig. 1 shows the  $^{13}\text{C}$  NMR spectrum of 600 °C pyrolysed fibres compared with the spectra of the precursor

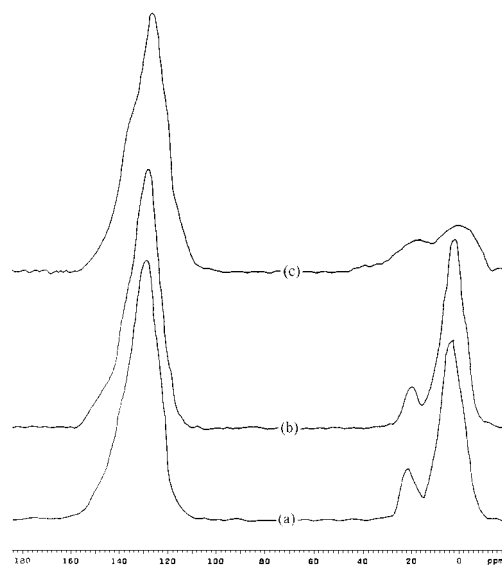


Figure 1  $^{13}\text{C}$  NMR spectrum of fibres after pyrolysis at 600 °C for 2 hours under argon compared with the spectra of precursor fibres and stabilized fibres (a) precursor fibres (b) stabilized fibres (c) pyrolysed fibres.

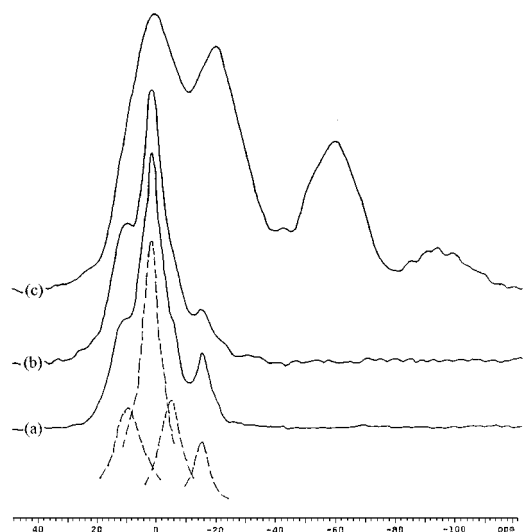


Figure 2  $^{29}\text{Si}$  NMR spectrum of fibres after pyrolysis at 600 °C for 2 hours under argon compared with the spectra of precursor fibres and stabilized fibres (a) precursor fibres (b) stabilized fibres (c) pyrolysed fibres.

and stabilized fibres. The peak around 3 ppm is assignable to aliphatic carbons bonded to silicon, which is drastically diminished on pyrolysis indicating the decomposition of the methyl side chain bonded to the silicon. The peak around 21 ppm due to methyl attached to aromatic rings also decreased but the peak around 129 ppm ascribed to aromatic carbons displays no appreciable changes indicating the stability and predominant presence of the aromatic carbons. Fig. 2 presents the  $^{29}\text{Si}$  NMR spectra of the various fibres. In the “as-spun” precursor fibre spectrum, the peak at  $-16.6$  ppm is assigned to silicon atoms bonded with one hydrogen and three carbon atoms ( $\text{SiC}_3\text{H}$ ), and the peak around 0.4 ppm is due to silicon atoms bonded only with aliphatic carbon atoms ( $\text{SiC}_4$ ), which has two shoulder peaks centred around 8 ppm and  $-6$  ppm (see the deconvoluted spectrum) respectively. The former is ascribed to silicon atoms bonded to one oxygen atom ( $\text{SiOC}_3$ ), whilst the latter is probably due to silicon atoms bonded to one aromatic carbon.

The presence of the  $\text{SiOC}_3$  implies the occurrence of partial oxidation during preparation and spinning of the precursor. The spectrum of the stabilized fibres displays a slight increase of the peak corresponding to silicon atoms bonded to one oxygen atom ( $\text{SiOC}_3$ ), and an appreciable decrease of that due to the silicon atoms bonded with one hydrogen and three carbon atoms ( $\text{SiC}_3\text{H}$ ). The shoulder peak in the spectrum of stabilized fibres at approximately  $-19$  ppm is assignable to a silicon atom attached to two oxygen atoms ( $\text{SiC}_2\text{O}_2$ ). The appearance of the spectrum of the stabilized fibres shows little change because the sample was stabilized to low extent, with a weight gain of only  $\sim 4.5$  wt % and the structural changes to the aromatic units are not reflected by the silicon spectrum. However, after the stabilized fibres were heat-treated at 600 °C for two hours and the aliphatic side chains and oxygen functional groups were reduced, the chemical bonding information of the Si-O structures were clearly revealed by the  $^{29}\text{Si}$  NMR spectrum. The peak assignable to silicon atom bonded to one oxygen atom ( $\text{SiOC}_3$ ) may be overlapped by the  $\text{SiC}_4$

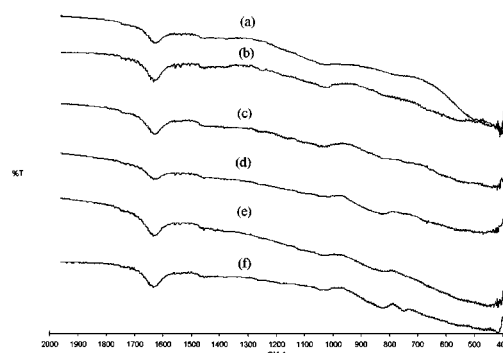


Figure 3 FTIR spectra of CSA fibres (stabilized to the weight gain of  $\sim 4.5$  wt %) after pyrolysis for 2 hours under argon at various temperatures. (a) 1000 °C (b) 1200 °C (c) 1300 °C (d) 1400 °C (e) 1500 °C (f) 1600 °C.

peak, but the peaks ascribed to silicon atoms in  $\text{SiC}_2\text{O}_2$ ,  $\text{SiCO}_3$  and  $\text{SiO}_4$  are clearly displayed in the spectrum.

The pyrolysis between 800 °C–1200 °C involves further condensation and loss of some hydrogen and methane gases accompanied by densification of the structure. Above the pyrolysis temperature of 1000 °C, the structural changes were studied by FTIR. Fig. 3 reveals the FTIR spectra of the carbon-silicon alloy (CSA) fibres (stabilized to the weight gain of  $\sim 4.5$  wt %) after pyrolysis for 2 hours under argon atmosphere at various temperatures. The spectrum of fibres pyrolysed at 1000 °C still shows a band at approximately  $490\text{ cm}^{-1}$  assignable to Si-O absorption. All the spectra show strong absorption bands at approximately  $1620\text{ cm}^{-1}$  ascribed to the C=C stretching vibration of the aromatic rings, indicating again the dominant existence of the carbon-rich structural characteristics of the fibres. It was not certain by FTIR analysis whether Si-C bonds were also present, since the associated absorption overlapped Si-O absorption at about  $800\text{ cm}^{-1}$  and  $1100\text{ cm}^{-1}$ . However, for fibres heat-treated above 1300 °C, the FTIR spectra showed the increasing absorption band at about  $820\text{ cm}^{-1}$ , which could be attributed to the formation of crystalline silicon carbide [8].

While the localized arrangements of atoms can be detected using FTIR spectroscopy, XRD is widely recognised as a better technique for examination of long range atomic ordering in a material. Fig. 4 displays X-ray ( $\text{CuK}\alpha$ ) diffraction patterns of CSA fibres (stabilized to the weight gain of  $\sim 4.5$  wt %) after pyrolysis for 2 hours under argon atmosphere at various

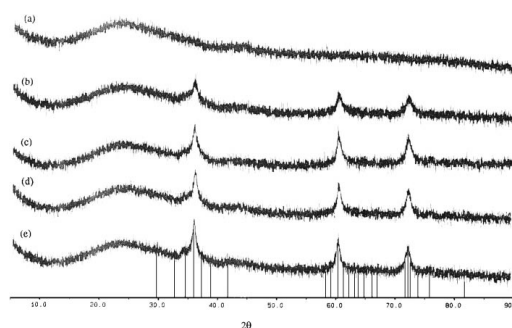


Figure 4 XRD traces of CSA fibres (stabilized to the weight gain of  $\sim 4.5$  wt %) after pyrolysis for 2 hours under argon at various temperatures. (a) 1200 °C (b) 1300 °C (c) 1400 °C (d) 1500 °C (e) 1600 °C.

TABLE I Mean grain size of  $\beta$ -silicon carbide as a function of pyrolysis temperature

Pyrolysis temperature/ $^{\circ}\text{C}$	1300	1400	1500	1600
Grain size (nm)	$\sim 3.5$	$\sim 5.5$	$\sim 9.5$	$\sim 11.5$

temperatures. The XRD pattern of the CSA fibres pyrolysed at  $1200^{\circ}\text{C}$  shows a very broad band at  $2\theta$  angle of about  $23^{\circ}$ , and indicates the paracrystalline state of the carbon structure. The XRD patterns of CSA fibres pyrolysed at  $1300^{\circ}\text{C}$  and above, show the distinctive band at approximately  $36^{\circ}(2\theta)$  accompanied by two bands at about  $60^{\circ}$  and  $72^{\circ}$  respectively, which indicate the presence of crystalline  $\beta$ -silicon carbide. From the XRD trace (Fig. 4), the width of the (111) peak located at  $2\theta$  angle of ca  $36^{\circ}$  was used to calculate the mean crystallite size of the  $\beta$ -silicon carbide in the CSA fibres. This was estimated according to Scherrer's equation with the results listed in Table I, which show that the mean crystalline grain size grows slowly from  $1300^{\circ}\text{C}$  to  $1400^{\circ}\text{C}$ , and more rapidly above  $1400^{\circ}\text{C}$ .

It is interesting to note that the stabilization degree strongly affects the crystalline transition process. It was found that the CSA fibres stabilized to the weight gain of  $\sim 10$  wt % after pyrolysis for 2 hours under argon atmosphere above  $1300^{\circ}\text{C}$  showed no crystallization of the SiC.

Fig. 5 shows that the XRD pattern of the CSA fibres stabilized to the weight gain of  $\sim 10$  wt % and pyrolysed at  $1300^{\circ}\text{C}$  is similar to that of the CSA fibres stabilized to the lower weight gain of  $\sim 4.5$  wt % and pyrolysed at  $1200^{\circ}\text{C}$ . It is believed that the large amount of Si-O bonding introduced by the excessive stabilization suppressed the crystallization of  $\beta$ -silicon carbide. The abundance of the Si-O structures in excessively stabilized CSA fibres is demonstrated by the FTIR spectra presented in Fig. 6. The excessively stabilized CSA fibres have a weaker band at  $\sim 1600\text{ cm}^{-1}$  indicating the lower concentration of the aromatic C=C, possibly because of carbon burn-off during the severe stabilization process. They also display a broad band at  $\sim 1020\text{ cm}^{-1}$  and a strong band at  $\sim 525\text{ cm}^{-1}$  probably arising from Si-O with a noticeable shoulder at  $\sim 800\text{ cm}^{-1}$ . Overall, the CSA fibres stabilized to the weight gain of  $\sim 4.5$  wt % show less intense Si-O absorption peaks.

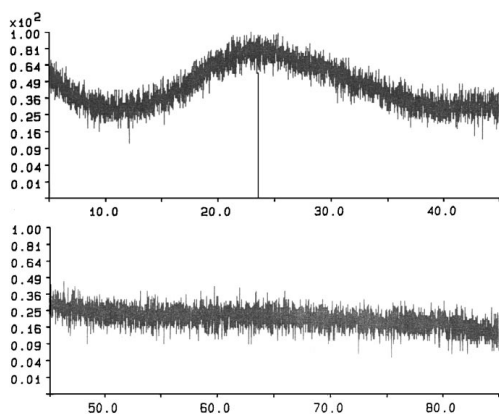


Figure 5 XRD trace of CSA fibres (stabilized to the weight gain of  $\sim 10$  wt %) after pyrolysis for 2 hours under argon at a temperature of  $1300^{\circ}\text{C}$ .

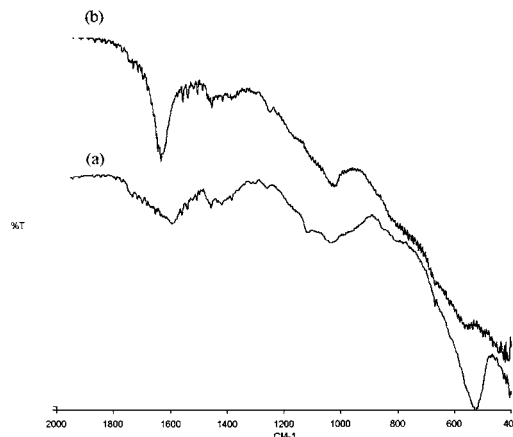


Figure 6 FTIR spectra of CSA fibres stabilized to different extents and pyrolysed at  $1200^{\circ}\text{C}$ . (a) Stabilized to the weight gain of  $\sim 10$  wt % (b) stabilized to the weight gain of  $\sim 4.5$  wt %.

### 3.2. Mechanical properties of the fibres

The strong impact of the degree of stabilization on the tensile properties of the resultant carbon-silicon alloy fibres is illustrated in Figs 7–9. Both the tensile strength and modulus of the pyrolysed fibres, irrespective of the stabilization degree, increase with the pyrolysis temperature (Figs 7, 8), reaching a maximum value at about  $1200^{\circ}\text{C}$ .

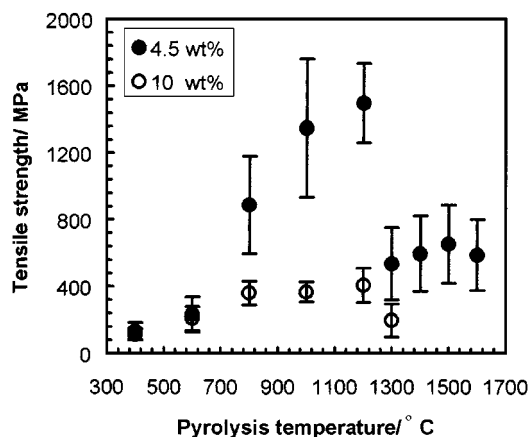


Figure 7 Tensile strength of CSA fibres as a function of pyrolysis temperature.

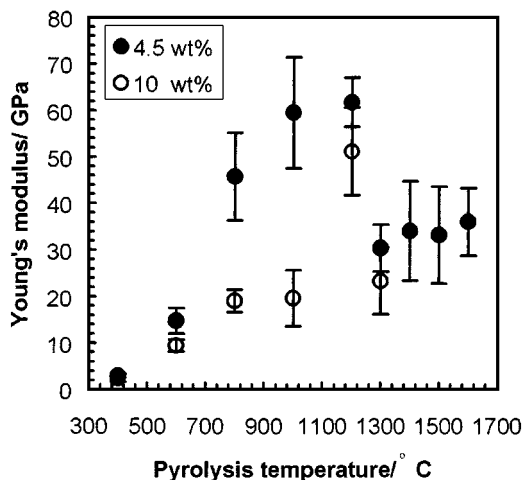


Figure 8 Young's modulus of CSA fibres as a function of pyrolysis temperature.

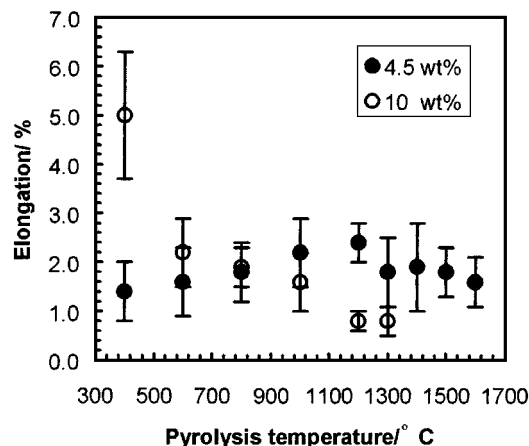


Figure 9 Relation between fracture elongation of CSA fibres and pyrolysis temperature.

Young's modulus increases in both cases, due to the structural change from the basic molecular solid to continuous C-C-Si-O bonded inorganic material. However, the stronger cross-linking in the highly oxidized sample leads to the very high failure strain. As this oxygen is gradually eliminated during pyrolysis the failure strain is reduced. The modulus does not increase between 800 °C and 1000 °C for the highly oxidized fibres. This could be because some oxygen is lost in this region. The tensile strength also stabilizes in this region for the highly oxidized fibres, consistent with the modulus. Thus, it could be that porosity is developing in the fibres. The lower oxygen content in the other fibre means that there is lower porosity created, and therefore Young's modulus and strength gradually increase.

The tensile strengths of the CSA fibres with different degrees of stabilization are strikingly different. The tensile strength of the CSA fibres with the greater stabilization degree (i.e., stabilized to the weight gain of ~10 wt %) appears to be constant in the region 600–1000 °C, whilst that of the fibres with the lower extent of stabilization sharply increases by a factor of more than 3. This is probably because the CSA fibres with a greater stabilization degree have more defects introduced by carbon burn-off during the excessive stabilization process. It is also possible that the defects were introduced in the early stage of the pyrolysis, during which more oxygen-containing groups were eliminated, leaving behind more severe defects that control the strength as the inorganic ceramic structure develops. In both cases, the tensile properties decrease sharply above a pyrolysis temperature of 1200 °C. The reason for the abrupt strength decrease is probably due to the oxygen loss in both fibres caused by internal chemical reaction forming CO gas and increasing the flaw size and population in the fibre structure [9]. For the CSA fibres stabilized to the weight gain of ~4.5 wt %, the crystallization of  $\beta$ -silicon carbide is another factor contributing to the abrupt tensile strength decrease. Another important point to mention is that the tensile strength of the CSA fibres stabilised to the weight gain of ~10 wt % became so small that it was almost impossible to measure when the pyrolysis temperature was raised to 1400 °C and above, but that of the CSA fibres stabilized to the weight gain of ~4.5 wt % became constant at close to

600 MPa when the pyrolysis temperature rose to the region of 1300–1600 °C. This suggests a marked increase in population of larger flaws in the former case, presumably due to the chemical reactions between more residual oxygen and carbon, and unchanged flaw sizes in the latter case because the oxygen was already consumed at 1300 °C. The oxygen content of fibres stabilized to the weight gain of ~10 wt % and pyrolysed at 1200 °C was more than two times of that of fibres stabilized to the weight gain of ~4.5 wt % and pyrolysed at 1200 °C.

The fracture elongation (Fig. 9) of the CSA fibres stabilized to the weight gain of ~10 wt % decreases steadily with the increase in pyrolysis temperature and reaches <1% at 1300 °C, whereas that of the CSA fibres stabilized to the weight gain of ~4.5 wt % slightly increases from 600 °C to 1200 °C and then decreases. Generally from 1200 °C to 1600 °C it maintains a steady value around 2%. This is probably because in the former case the stabilized fibres had a fracture strain of ~5% due to oxygen cross-links. Most of the excessive oxygen atoms survived the early stage of the pyrolysis process (400 °C–800 °C) and remained as Si-O bonds which when converted to amorphous silica formed a more brittle structure with increasing pyrolysis temperature. In the latter case, however, the stabilized fibres had a low fracture strain (<1%) because there were fewer oxygen cross-links in the structure and only a small number of Si-O bonds existed. In this case, the fracture strain of the fibres increased as the structure developed when the pyrolysis temperature was increased up to 1200 °C. However, above 1300 °C the structure became more brittle as the crystalline grain size increased.

### 3.3. Electrical resistance of the CSA fibres

Fig. 10 shows the specific resistivity of the CSA fibres as a function of pyrolysis temperature, compared with silicon carbide fibres (Nicalon<sup>®</sup>) and PAN carbon fibres. It is evident that the specific resistivity of the CSA fibres is between those of the silicon carbide fibres and the PAN carbon fibres. This is because of the composition of the CSA fibres, and the aromatic carbon structure. The fact that the electrical resistivity of the

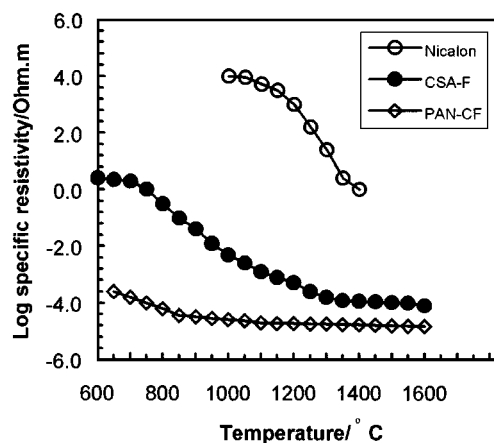


Figure 10 The specific resistivity of CSA fibres as a function of pyrolysis temperature, compared with SiC fibres (Nicalon<sup>®</sup>) and PAN carbon fibres.

CSA fibres is higher than that of the PAN fibres is due to two factors: (1) the volume fraction of carbon is less than that of PAN fibres, and (2) the aromatic carbon layers are randomly oriented whereas for the PAN fibres they are highly oriented along the fibre axis. The specific electrical resistivity of the CSA fibres decreases as the pyrolysis temperature increases, the abrupt drop between 800–1000 °C indicating the substantial structural change taking place in this temperature region. When the pyrolysis temperature rises to 1200 °C and above, the electrical resistivity gradually decreases and stabilizes at approximately  $1.2 \times 10^{-4} \Omega\text{m}$ . Compared to the silicon carbide fibres, the specific electrical resistivity of the CSA fibres is lower by about 4 orders of magnitude. In contrast, the specific electrical resistivity of the PAN carbon fibres shows almost no change in the temperature range 800–1600 °C.

### 3.4. Oxidation resistance and control oxidation process

Fig. 11 shows the thermogravimetric analysis of various fibres up to 1000 °C in air at a heating rate of 5 °C/min. The pitch-based carbon fibres began to oxidize at around 440 °C, showed vigorous oxidation at ~550 °C and were completely oxidized at close to 700 °C. In contrast, the CSA fibres behaved in the same way below 550 °C due to the initial carbon oxidation, but at 550 °C where the pitch-based carbon fibres showed extremely rapid burn-off, the CSA fibres lost weight only slowly. This was probably due to the simultaneous silica formation, which partly balanced the weight loss and slowed down the oxidation process. The CSA fibres gradually reached a maximum weight loss of about 40 wt %, attained at 900 °C, and thus appear more oxidation resistant than the carbon fibres. The net weight loss that would result if the carbon is completely oxidized and the silicon is fully converted into silica is shown in the figure. It can be seen that the CSA fibre weight loss curve reaches this point indicating that they are converted into silica fibres.

The residual fibres after oxidation to 1000 °C are white because of the removal of the carbon phase. The SEM observation reveals that these residual CSA fibres maintain their fibrous morphology and have a uniform

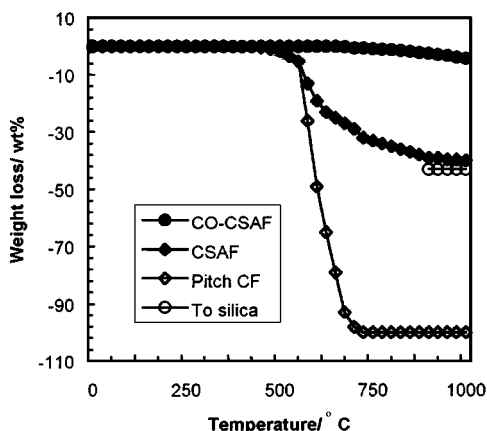


Figure 11 Thermogravimetric analysis of various fibres (in air, 5 °C/min).

glassy structure with no visible pores after the removal of the carbon phase, suggesting that silicon and the carbon phase were originally mixed homogeneously at the molecular level. The CSA fibres may have improved the oxidation resistance by providing a diffusion barrier to oxidation, but obviously the barrier is permeable because the carbon burn-off left channels for oxygen and the resultant silica was not mobile enough at the temperatures used to block the channels. This analysis holds out a possibility that oxidation at higher temperature may form an impermeable oxidation barrier due to the improved mobility of silica.

To test this hypothesis, the CSA fibres were heated to 1200 °C under an argon atmosphere and then exposed to oxygen for a short period of time (<10 min). As a result the fibres obtained exhibited a remarkably improved oxidation resistance, presumably because an impermeable silica layer developed at the outer surface of the fibres. This process could be carried out during pyrolysis at 1200 °C by adding oxygen into the argon stream at the end of the process. These fibres are called control oxidized carbon-silicon alloy fibres (CO-CSA fibres). Fig. 11 shows the oxidation behaviour of the CO-CSA fibres, which do not show any oxidative weight loss until 700 °C, and the overall weight loss at 1000 °C is less than 5 wt %.

A series of control oxidation experiments were carried out to introduce the required silica layer. During the control oxidation process, the different conditions have a bearing on the oxidation resistance of the resultant fibres. For example, stabilized fibres were pyrolysed in an argon gas stream, at a heating rate of 100 °C/hr up to 1200 °C. At 1200 °C oxygen was added to partially and quickly oxidize the fibres for a short period of time. The oxidation resistance of the resultant fibres is shown in Fig. 12. For the same oxidation time, the increase of oxygen flow rate improves the oxidation resistance. In the case of the same oxygen flow rate, a short oxidation time gives a more oxidation resistant result. The SEM observations showed that the CO-CSA fibres have smooth outer surfaces similar to those of the CSA fibres. The protective outer layer which was expected to be a silica coating was seldom observed under SEM imaging. However, the existence of the silica layer can be proved by EDX analysis of the surface and the internal area of the fibre, showing that the surface has a

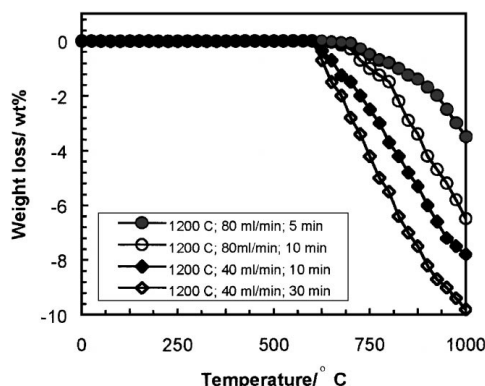


Figure 12 Comparison of oxidation resistance of CO-CSA fibres obtained under different control oxidation conditions.

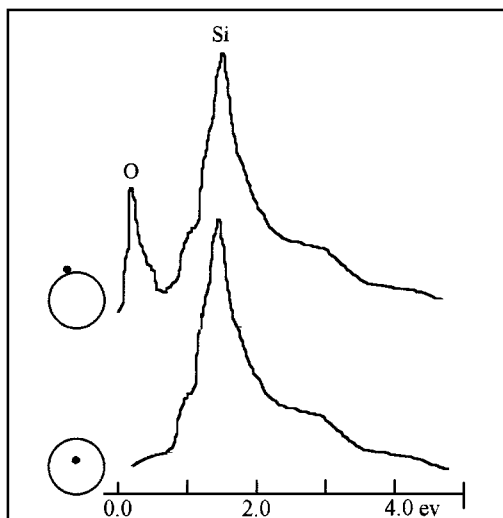


Figure 13 EDX analysis of the surface and internal area of CO-CSA fibre.

significant oxygen peak, whereas there is no appreciable oxygen detectable in the internal area (Fig. 13). When measuring the electrical resistance of the CO-CSA fibres, it was noted that the outer surface acts like an insulator but the inside has a resistivity value typical of carbon-silicon alloy fibres. This is also good evidence for the presence of the silica outer layer. The absence of a clearly discernible silica layer suggests that there is not a clear-cut visible interface between the protective layer and the inside structure of the CO-CSA fibres. This could be beneficial to the fibres since the layer will not behave like an artificial coating that tends to crack in use.

It is believed that the control oxidation reaction forms a thin silica layer, due to the higher mobility of  $\text{SiO}_2$  at this temperature. This layer acts as an impermeable barrier to the oxidation and protects the internal structures when exposed to air.

Interestingly, the silica layer introduced during the control oxidation process enhances the thermal stability of the whole fibre. Fig. 14 shows the comparison of oxidation resistance of CO-CSA fibres with CSA fibres obtained under different conditions. The CSA fibres pyrolysed at  $1350^\circ\text{C}$  have almost 10% higher weight loss than the CSA fibres pyrolysed at  $1200^\circ\text{C}$ , possibly because the CSA fibres pyrolysed at  $1350^\circ\text{C}$  experienced the reaction given in Equation 1, in which

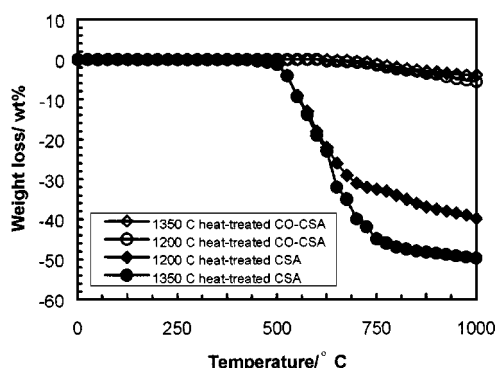
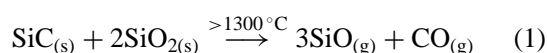


Figure 14 Comparison of oxidation resistance of CO-CSA fibres obtained under different control oxidation conditions.

silicon is removed in an atomic ratio of 3 : 1 to carbon, resulting in relatively lower silicon content. As a result, the CSA fibres have very low tensile properties due to the additional flaws, and when exposed to air, the carbon phase can be burnt off and silicon converted into silica, the lower silicon content leading to higher weight loss. In contrast, when the CO-CSA fibres (control oxidation at  $1200^\circ\text{C}$ ) were heated to higher than  $1300^\circ\text{C}$ , the internal reaction might occur according to Equation 1, but the reaction products [ $\text{SiO}_{(g)}$  and  $\text{CO}_{(g)}$ ] had to diffuse out through the silica outer layer which was difficult due to the impermeability of the silica layer. Thus the reaction was suppressed. Therefore the CO-CSA fibres heat-treated at  $1350^\circ\text{C}$  do not show the decreased oxidation resistance but instead have slightly improved oxidation resistance, probably due to a better sealing of the silica layer at the higher heat treatment temperature.



The CO-CSA fibres after being exposed to air at  $1000^\circ\text{C}$  for 20 hours still maintain approximately 70% of the initial tensile strength. The decrease in tensile strength was largely attributed to the defects of the outer silica layers, which were caused by the original fibre defects such as cracks and voids and particle inclusions. These defects could not be removed by the control oxidation; on the contrary, they remained as flaws in the CO-CSA fibres.

Fig. 15 shows the FTIR spectrum of the CO-CSA fibres compared with those of the CSA fibres and CO-CSA fibres after oxidation at  $1000^\circ\text{C}$  for 20 hours. Although the FTIR spectra only reflect the structure of bulk fibres, the intensity increase of the bands at  $1100\text{ cm}^{-1}$ ,  $790\text{ cm}^{-1}$  and  $\sim 490\text{ cm}^{-1}$  of the CO-CSA fibre spectrum could be attributed to the formation of the silica layer. It can be seen that CO-CSA fibres have more silica than CSA fibres. The further increase in intensity of the above three bands in the spectrum of CO-CSA fibres after oxidation at  $1000^\circ\text{C}$  for 20 hours indicates the increase of the silica content.

Fig. 16 shows the FTIR spectrum of the CO-CSA fibres compared with those of the fibres after oxidation under different conditions. The intensities of the bands at  $1100\text{ cm}^{-1}$ ,  $790\text{ cm}^{-1}$  and  $490\text{ cm}^{-1}$  reflect



Figure 15 FTIR spectra of CSA fibres, CO-CSA fibres and CO-CSA fibres after oxidation at  $1000^\circ\text{C}$  in air for 20 hours (a) CSA fibres (stabilized to the weight gain of  $\sim 4.5\text{ wt}\%$ , and pyrolysed at  $1200^\circ\text{C}$  in argon) (b) CO-CSA fibres [fibres (a) after controlled oxidation] (c) CO-CSA fibres after oxidation [fibres (b) exposed to air at  $1000^\circ\text{C}$  for 20 hours].

TABLE II The properties of some CO-CSA fibres

Stabilization extent (weight gain wt %)	CSA fibres			CO-CSA fibres			CO-CSA fibres wt loss in air at 1000 °C
	$\sigma$ MPa	E GPa	$\epsilon$ %	$\sigma$ MPa	E GPa	$\epsilon$ %	
~10 wt %	350	28	1.3	310	33	0.9	4.8 wt %
~4.5 wt %	1170	50	2.5	810	63	1.3	3.5 wt %

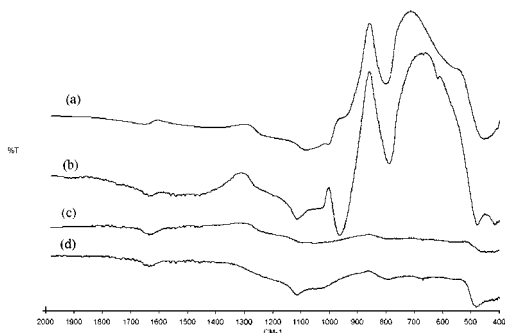


Figure 16 FTIR spectra of CSA fibres and CO-CSA fibres after oxidation under different conditions (a) CSA fibres after oxidation in air at 500 °C for 200 hours (b) CSA fibres after oxidation in air at 1000 °C (heating rate 5 °C/min) (c) CO-CSA fibres (d) CO-CSA fibres after oxidation in air at 1000 °C for 20 hours.

the amount of silica present in the fibres. Evidently, only a fraction of the CO-CSA fibre structure is silica [spectrum (c)] even after oxidation at 1000 °C [spectrum (d)], compared with those of the CSA fibres which have been converted to silica to a greater extent [spectra (a) and (b)].

The tensile properties of the CO-CSA fibres depend mainly on the characteristics of the spinning precursor, spinning conditions, stabilization extent and control oxidation conditions. The influence of the stabilization extent and control oxidation conditions are summarised and listed in Table II, revealing that the tensile strength of CO-CSA fibres is slightly inferior to that of the carbon-silicon alloy fibres obtained under identical circumstances, but Young's modulus increases by a factor of 20% due to the introduction of the impermeable silica layer. This implies that the control oxidation reaction introduces a small number of additional flaws or slightly increases the size of the existing defects. However, the CO-CSA fibres have improved thermal stability and electrically insulative surface as well as the advantages of carbon fibres. Extended application areas can be envisaged. In addition to the above advantages, the CO-CSA fibres can withstand high temperatures. After heat treatment at temperatures above 2700 °C, they maintain their fibre integrity. Presumably it is the carbon phase which maintains the structural configuration of fibres.

#### 4. Conclusion

When the CSA fibres were heated to 1200 °C under an argon atmosphere and then exposed to oxygen for a short period of time, an oxidation resistant silica layer was formed on the surface of the fibres. This process is called control oxidation, in which presumably oxygen quickly oxidized the fibre surface, removed the carbon

phase and converted the silicon into silica that sealed the channels left by the carbon burn-off. This process is effective provided that the temperature is high enough so that the silica is mobile and there is an even distribution of carbon and silicon at the molecular level. The presence of the silica layer was indirectly proved by EDX analysis of the surface and the internal area of the fibre, showing that the surface has more oxygen than the internal area. The electrically insulative surface also indicates the existence of the silica layer. The tensile strength of the CO-CSA fibres was reduced by 20% during the control oxidation process. The oxidation resistance of CO-CSA fibres was greatly improved compared with carbon fibres. The CO-CSA fibres after oxidation at 1000 °C for 20 hours only show a slight increase of the silica content, which in turn gives rise to a further decrease in tensile strength by approximately 30%. However, there were no outer layer cracks as experienced by the protective coating of the carbon fibres in use, and no noticeable additional structural flaws were observable under SEM. This holds out the possibility of better performance of the CO-CSA fibres by reducing the defects of the original fibres through improving spinning equipment and optimising stabilization conditions.

#### Acknowledgement

The authors wish to thank the EPSRC solid-state NMR service in Durham University for solid state <sup>13</sup>C and <sup>29</sup>Si NMR analysis, and S. Lu gratefully acknowledges the financial support from the University of Leeds, School of Chemistry and Department of Materials.

#### References

1. W. WEISWEILER and G. NAGEL, in *Carbon '86* (Ext. Abstr.) Baden-Baden (Deut. Keram. Ges.), 1986, p. 646.
2. H. HANNACHE, J. QUENISSET, R. NASLAIN and L. HERAUD, *J. Mat. Sci.* **19** (1984) 202.
3. W. P. HOFFMAN, H. T. PHAN and A. GROSZEK, *Carbon* **33** (1995) 509.
4. J. W. FERGUS and W. L. WORRELL, *Carbon* **33** (1995) 537.
5. S. YAJIMA, J. HAYASHI and M. OMORI, *Chem. Lett.* **9** (1975) 931.
6. S. LU, B. RAND, K. D. BARTLE and A. W. REID, *Carbon* **35** (1997) 1485.
7. S. LU, B. RAND and K. D. BARTLE, *submitted to J. Mat. Res.*
8. W. G. SPITZER, D. KLEINMAN and D. WALSH, *Physical Review* **113** (1959) 127.
9. S. M. JOHNSON, R. D. BRITAIN, R. H. LAMOREAVX and D. J. ROWCLIFF, *J. Am. Ceram. Soc.* **71**[3] (1988) C-132.

Received 17 April  
and accepted 21 August 1998